

Electron Confinement in Structurally Constrained σ -Bonded π -Systems. An Experimental and Density Functional Investigation

Angelika Niemz,[†] Alejandro Cuello,[†] L. Kraig Steffen,[‡] Benjamin F. Plummer,[§] and Vincent M. Rotello^{*,†}

Contribution from the Department of Chemistry, University of Massachusetts, Amherst, Massachusetts 01003, Department of Chemistry, Fairfield University, Fairfield, Connecticut 06430, and Department of Chemistry, Trinity University, San Antonio, Texas 78212

Received December 17, 1999. Revised Manuscript Received March 27, 2000

Abstract: We have explored the effect of resonance overlap on electronic communication in σ -bonded π -systems through a combined experimental and computational investigation. The system studied consists of a series of diphenyl-substituted acenaphthofluoranthenes and fluoranthenes with constrained dihedral angles between polycyclic core and phenyl substituents of 90°, 70°, and 15°. The spin density distribution within the radical anions of these conformationally restricted polycyclic aromatic hydrocarbons was assessed via DFT-B3LYP calculations validated through SEEPR-derived experimental hyperfine coupling constants (hfc's). Orthogonal subsystems were essentially insulated, while substantial delocalization of spin density was observed for near-planar subsystems. The insulation of the phenyl substituents combined with the possibility of forming ladder-type polymers makes the orthogonal diphenyl-substituted acenaphthofluoranthenes intriguing building-blocks for molecular electronics.

Introduction

Electronic communication through π -bonds plays a key role in the creation of molecular electronic devices.^{1,21,2} Extended π -conjugation in molecular wires provides a low-energy path for long-range intramolecular electron transfer.^{3–5} The bonding and antibonding π -orbitals in these systems are delocalized into conduction and valence bands with a relatively small band gap, analogous to semiconductors.⁶ Localized states in the form of uncoupled π -systems, on the other hand, are desirable in the quest for molecular quantum effect devices⁷ and organic ferromagnets.^{8,9,9} One approach to such electron confinement makes use of the dependence of electron delocalization on the dihedral angle θ between σ -bonded π -systems. For θ approaching 90° (orthogonal π -systems) molecular orbital theory predicts the overlap integral S_{ij} between two σ -bonded π -systems to approach zero, rendering insulated subsystems.¹⁰ Isolation of orthogonal, spin-carrying subunits in a series of oligo (9,10-anthrylene)s indeed led to the generation of high-spin polyradical

anions.⁹ These systems were found, however, to possess a singlet ground state, and it was proposed that better isolation through more rigid orthogonal alignment is necessary for the generation of true organic ferromagnets. Hyperconjugation between orthogonal π -systems further contributes to the observed residual spin delocalization. EPR, ENDOR, and TRIPLE spectroscopy of 9,10-diphenylanthracene^{11,12,11} and rubrene¹³ have shown substantial hfc's associated with the meta-position of the phenyl substituents. INDO calculations for this phenyl hyperconjugation predict a $\sin^2 \theta$ dependence of the meta-proton hfc on the spin density of the carbon atom, to which the phenyl ring is attached.^{11,14} Since the 9,10 positions of the anthracene radical anion are the centers of highest spin density, substantial spin density delocalization into the phenyl substituents of 9,10-diphenylanthracene is to be expected. Better isolation between σ -bonded π -systems is predicted if the phenyl substituents are connected at sites of low spin density. Two systems which fulfill such a requirement are 7,14-disubstituted acenaphtho[1,2-*k*]fluoranthenes and 7,10-disubstituted fluoranthenes. The radical anions of these nonalternant polycyclic aromatic hydrocarbons possess comparatively small spin densities at the substitution positions (vide infra),¹² combined with steric hindrance between core and phenyl substituents, which causes an out-of-plane rotation of the latter.

We here report a combined EPR-spectroelectrochemical and computational investigation of the spin density distribution within the one-electron reduced radical anions of 7,14-disubstituted acenaphtho[1,2-*k*]fluoranthenes **1a–c** as well as 7,10-

[†] University of Massachusetts.

[‡] Fairfield University.

[§] Trinity University.

(1) *Molecular Electronics*; Jortner, J., Ratner, M., Eds.; Blackwell Science: Oxford, 1997.

(2) *Molecular Electronics and Molecular Electronic Devices*; Siemicki, K., Ed.; CRC Press: Boca Raton, FL, 1992; Vols. 1–3.

(3) Tour, J. M. *Chem. Rev.* **1996**, *96*, 537–553.

(4) Tolbert, L. M.; Zhao, X.; Ding, Y.; Bottomley, L. A. *J. Am. Chem. Soc.* **1995**, *117*, 12891–12892.

(5) Swager, T. M. *Acc. Chem. Res.* **1998**, *31*, 201–207.

(6) Schmidt, A.; Armstrong, N. R.; Goeltner, C.; Muellen, K. *J. Phys. Chem.* **1994**, *98*, 11780–11785.

(7) Goldhaber-Gordon, D.; Montemero, M. S.; Love, C.; Opiteck, G. J.; Ellenbogen, J. C. *Proc. IEEE* **1997**, *85*, 521–540.

(8) Tyutyulkov, N. *Pure Appl. Chem.* **1996**, *68*, 345–352.

(9) Mueller, U.; Baumgarten, M. *J. Am. Chem. Soc.* **1995**, *117*, 5840–5850.

(10) Heilbronner, E.; Bock, H. *The HMO-Model and its Applications*; Wiley: New York, 1976.

(11) Biehl, R.; Hinrichs, K.; Kurreck, H.; Lubitz, W.; Mennenga, U.; Roth, K. *J. Am. Chem. Soc.* **1977**, *99*, 4278–4286.

(12) Grein, K.; Kirste, B.; Kurreck, H. *Chem. Ber.* **1981**, *114*, 254–266.

(13) Biehl, R.; Dinse, K. P.; Moebius, K.; Plato, M. *Tetrahedron* **1973**, *29*, 363–368.

(14) Pople, J. A.; Beveridge, D. L. *J. Chem. Phys.* **1968**, *49*, 4725–4762.

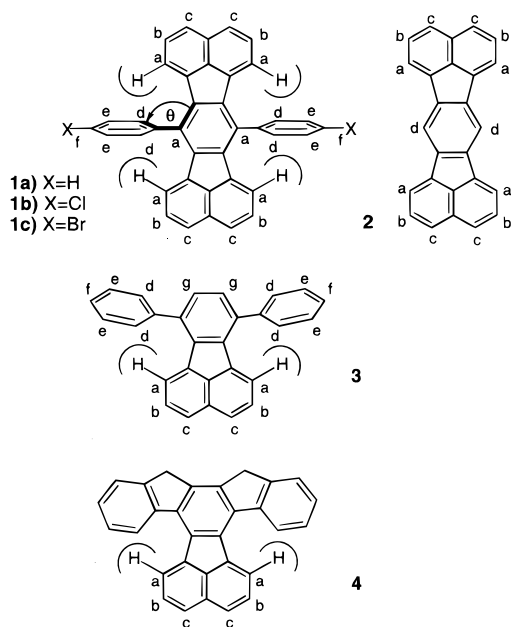


Figure 1. Conformationally restrained diphenyl-substituted acenaphthofluoranthenes **1a–c**, parent compound acenaphthofluoranthene **2**, diphenylfluoranthene **3**, and tied-back fluoranthene **4**. The positions of equivalent protons are labeled a–g.

diphenylfluoranthene **3** and the tied-back 8,9-dihydroindeno[1,2-*j*:2'-*l*]fluoranthene **4** (Figure 1).¹⁵ Recent interest in these systems has been sparked through the discovery that diphenyl acenaphthofluoranthene **1a** can undergo oxidative electropolymerization.¹⁶ Carbon–carbon bond formation involving the polycyclic core results in a ladder-type polymer with extended π -structure, which is electroactive and electrochromic. In the diphenyl acenaphthofluoranthene system, the σ -bonded phenyl substituents of the acenaphthofluoranthenes **1a–c** are forced into near-orthogonal orientation with respect to the polycyclic core as confirmed by the X-ray crystal structure of **1a**,¹⁷ due to steric interactions between the ortho-hydrogens of the phenyl substituents and the four buttressing hydrogens at positions 1, 6, 8, and 13 of the acenaphthofluoranthene moiety. The tied-back fluoranthene **4** serves as the other extreme: the bridging methylene groups restrain the dihedral angle between phenyl substituents and fluoranthene core to about 15°. For fluoranthene **3**, the average dihedral angle amounts to about 70°, due to the less sterically demanding polycyclic core, which allows for greater rotational freedom of the phenyl substituents combined with the possibility of an out-of-plane bend.

Fluorescence quenching experiments carried out to assess the intramolecular heavy atom effect of **1c** and the di-*p*-bromo analogues of **3** and **4** indicated a qualitative correlation between quantum yield and dihedral angle.¹⁵ Fluorescence quenching, i.e., communication between core and phenyl substituents in the excited state, ranged from negligible for the orthogonal acenaphthofluoranthene **1c** to almost complete for the near-planar dibromo analogue of **4**. We report here the quantitative determination of electron delocalization in the radical anion state for these structurally constrained polycyclic aromatic hydrocarbons using a combined EPR and computational strategy.

(15) Plummer, B. F.; Steffen, L. K.; Braley, T. L.; Reese, W. G.; Zych, K.; Van Dyke, G.; Tulley, B. *J. Am. Chem. Soc.* **1993**, *115*, 11542–11551.

(16) Debad, J. D.; Bard, A. J. *J. Am. Chem. Soc.* **1998**, *120*, 2476–2477.

(17) Watson, W. H.; Kashyap, R. P.; Plummer, B. F.; Reese, W. G. *Acta Crystallogr.* **1991**, *C47*, 1848–1851.

Experimental Section

Materials and General Methods. Solutions were prepared using reagent grade THF dried via distillation over sodium metal. Tetrabutylammonium perchlorate (TBAP, obtained from SACHEM, electro-metric grade) was recrystallized twice from water and dried for several days under high vacuum. Compounds **1a**,¹⁸ **1b–c**,¹⁵ **2**,¹⁸ **3**, and **4**¹⁹ were synthesized according to literature procedures.

Simultaneous Electrochemistry and EPR (SEEPR). Due to the lossy nature of the samples and to minimize perturbation of the microwave field by the working electrode, SEEPR experiments were carried out in a quartz flat cell. A second glass part containing three ACE #7 threaded joints sealed via Teflon ferrules to hold the electrodes and a septum capped ground glass joint for degassing and sample injection was connected to the top of the cell. The working electrode, a platinum gauze electrode, was inserted into the flat part of the cell. The Ag-wire pseudoreference electrode was positioned directly above the working electrode to minimize the iR -drop and the auxiliary electrode, a platinum wire spiral of large surface area, occupied the solvent reservoir above the flat section. The electrode leads were insulated via Teflon heat shrink tubing. After each experiment the working electrode was cleaned in concentrated HNO₃.

EPR spectra were recorded on an IBM ESP 300 X-band spectrometer equipped with a TE₁₀₄ dual cavity. Solutions of the polycyclic hydrocarbons (10⁻³ M in THF, 0.1 M TBAP) were degassed by bubbling argon through them for 5 min and then injected into the cell, which was previously flushed with argon. The cell was mounted within the spectrometer using custom manufactured cell holders, which allow for precise alignment of the cell within the cavity to maximize the Q-factor. Bulk electrolysis was carried out simultaneous to signal acquisition (25 kHz field modulation, modulation amplitude 0.0475 G). Hyperfine coupling constants (hfc's) were determined through spectrum simulation and iterative curve-fitting using the software package WinSim from NIEHS.²⁰ Excellent correlation (correlation coefficient greater than 0.99) was achieved in most cases.

Calculations

UHF and DFT-B3LYP calculations were performed using the Gaussian 94 suite of programs.²¹ UHF geometry optimization of the anion radicals at the 3-21G* level was followed by B3LYP/6-311G* single-point calculations, with DFT theoretical results showing little spin contamination for the systems under study.²² Isotropic hfc's were calculated according to:

$$a(N) = (8\pi/3)g_e\beta_e g_N\beta_N \rho(N)$$

The hfc of nucleus N, $a(N)$, is proportional to the corresponding fermi contact integral (spin density at the nucleus) $\rho(N)$; g_e (g_N) stands for the electronic (nuclear) g -factor and β_e (β_N) for the Bohr (nuclear) magneton.²³

Results and Discussion

Simultaneous electrochemistry and EPR (SEEPR) of acenaphthofluoranthenes **1a–c** and **2** and fluoranthenes **3** and **4** provided

(18) Tucker, S. H. *J. Chem. Soc.* **1958**, 1462.

(19) Dilthey, W.; Henkels, S. *J. Prakt. Chem.* **1937**, *85*, 85–97.

(20) NIEHS WinSim EPR, Duling, D., Laboratory of Molecular Biophysics, NIEHS, NIH, DHHS, 1994.

(21) Gaussian 94, Frisch, M. J.; Trucks, G. W.; Schlegel, H. B.; Gill, P. M. W.; Johnson, B. G.; Robb, M. A.; Cheeseman, J. R.; Keith, T.; Peterson, G. A.; Montgomery, J. A.; Raghavachari, K.; Al-Laham, M. A.; Zakrzewski, V. G.; Ortiz, J. V.; Foresman, J. B.; Cioslowski, J.; Stefanov, B. B.; Nanayakkara, A.; Challacombe, M.; Peng, C. Y.; Ayala, P. Y.; Chen, W.; Wong, M. W.; Andres, J. L.; Replogle, E. S.; Gomperts, R.; Martin, R. L.; Fox, D. J.; Binkley, J. S.; Defrees, D. J.; Baker, J.; Stewart, J. P.; Head-Gordon, M.; Gonzalez, C.; Pople, J. A., Gaussian, Inc.: Pittsburgh, PA, 1995.

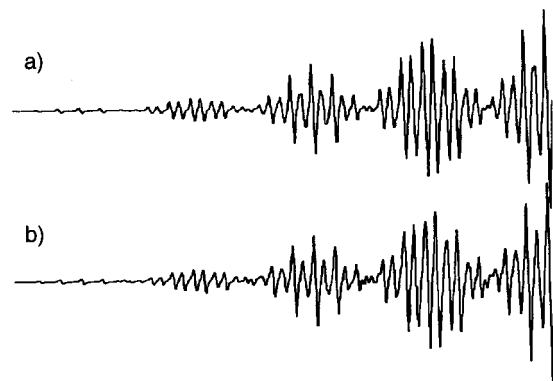
(22) S² at the B3LYP/6-311G*/UHF/3-21G* level before/after annihilation: **1a**, 0.778/0.751; **1b**, 0.778/0.751; **2**, 0.756/0.750; **3**, 0.764/0.750; **4**, 0.766/0.750.

(23) Koh, A. K.; Miller, D. J. *At. Data Nucl. Data Tables* **1985**, *33*, 235–253.

Table 1. Experimental and Calculated hfc's [G] for Radical Anions 1–4

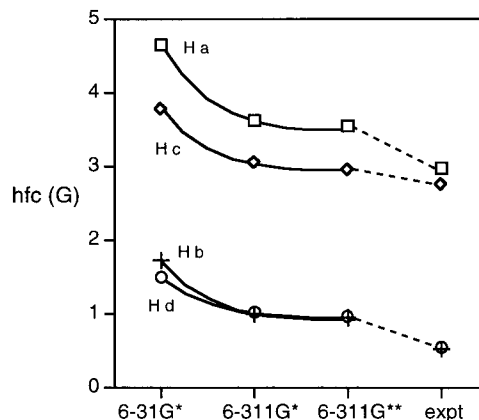
proton	1 ^{a,b}	1 ^b	1 ^c	2 ^{a,b}	3 ^{a,b}	4 ^{a,b}
Ha	2.77 (3.10)	2.79 (3.02)	2.79	2.73 (3.03)	4.15(4.53)	4.16 (4.23)
Hb	0.51 (0.94)	0.54 (0.86)	0.53	0.52 (0.98)	0.29 (0.98)	0.98 (0.87)
Hc	2.96 (3.54)	2.96 (3.47)	2.97	2.96 (3.61)	5.23 (5.78)	5.24 (5.42)
Hd	0.03(0.03)	0.04 (0.02)	0.00	0.53 (1.02)	0 (0.00)	0.22 ^d
He	0.04 (0.04)	0.00 (0.05)	0.00		0 (0.03)	0.21 ^d
X/H _f	0.01(0.02)				0.01 (0.05)	0.23 ^d
H _g					1.15 (1.41)	1.03 ^d

^a Experimental values obtained through curve fitting of the SEPR spectra. ^b Calculated hfc's (in parentheses) obtained using B3LYP/6-311G**/UHF/3-21G*. ^c Calculations were not run on 1c. ^d hfc's derived from spectral simulation, but not assigned to specific molecular positions (vide infra).

**Figure 2.** Low-field half of the EPR spectrum of the acenaphthofluoranthene 2 radical anion: (a) experimental, bulk electrolysis of 2 [10^{-3} M], 0.1 M TBAP carrier electrolyte, THF; and (b) simulated.

high-resolution spectra for the electrochemically generated radical anions. Proton hyperfine coupling constants (hfc's) were obtained via spectrum simulation and nonlinear least squares curve fitting (Table 1).²⁰ Very good correlation between experimental and simulated spectra was achieved (Figure 2). Curve-fitting of the EPR spectra for the buttressed diphenyl acenaphthofluoranthenes 1a–c indicated little spin density residing on the phenyl substituents as evidenced by the small hfc's for phenyl protons. Additionally, the hfc's of the core protons are essentially identical with those for the parent 2, indicating little perturbation of the core electronic structure due to the phenyl substituents. From the experimental hfc's it is apparent that for diphenyl fluoranthene 3 as well, most of the unpaired spin resides within the core. The radical anion of the essentially planar 4, on the other hand, exhibits appreciable hyperfine splitting caused by protons of the tied-back phenyl substituents, indicating more extensive electron delocalization.

The experimentally accessible hfc's can serve as a critical benchmark for the accuracy of computational results, which predict properties not directly accessible via simple EPR experiments, e.g. the spin density distribution within the π -framework. To correlate the experimental results with changes in spin densities, we carried out a series of DFT-B3LYP calculations. It is now widely recognized that calculations based on UHF wave functions overestimate spin densities and isotropic hfc's in π -radicals.^{24–26} While post-Hartree–Fock methods have been applied successfully to study small radicals, computational effort makes application to larger systems prohibitive.²⁴ In recent research, we²⁷ and other groups^{28–30} have shown the utility of

**Figure 3.** Calculated and experimental hfc's for acenaphthofluoranthene 2. Calculations were based on UHF/3-21G* geometry.

the B3LYP self-consistent hybrid functional in the prediction of spin density distribution and isotropic hfc's in organic π -radicals. To determine the proper choice of basis set for our system, we performed calculations at varying levels of theory. In previous studies, B3LYP/6-31G**/UHF/3-21G*-calculated hfc values have been shown to be in excellent agreement with experimental results.^{27,29} For the radical anion of acenaphthofluoranthene 2, we found that the B3LYP/6-31G* basis set gave somewhat overstated hfc's. Higher level B3LYP/6-311G*-calculated hfc's were in good agreement with the experimental values, with little improvement seen with the more computationally demanding B3LYP/6-311G** (Figure 3). Since experimental and calculated hfc's are in good agreement, the computational results can be used to predict properties for our systems not directly accessible via simple EPR experiments, e.g. the changes in spin density distribution within the π -framework.

Geometry optimization (UHF/3-21G*) of the buttressed diphenyl acenaphthofluoranthenes 1a,b showed the minimum energy conformation to have the phenyl rings perpendicular to the plane of the core. As with acenaphthofluoranthene 2, there was excellent agreement observed between the DFT-predicted and experimental hfc's (Table 1). Very little spin density was found to reside on the phenyl rings of 1a,b: 99% of the total spin density is localized in the core (Table 2). This value is quite constant for the analogous systems 1a,b, demonstrating independence between the electronic nature of the substituents and efficiency of communication.

For the less constrained diphenyl fluoranthene 3, the calculated structure for the anion radical has phenyl-core dihedral

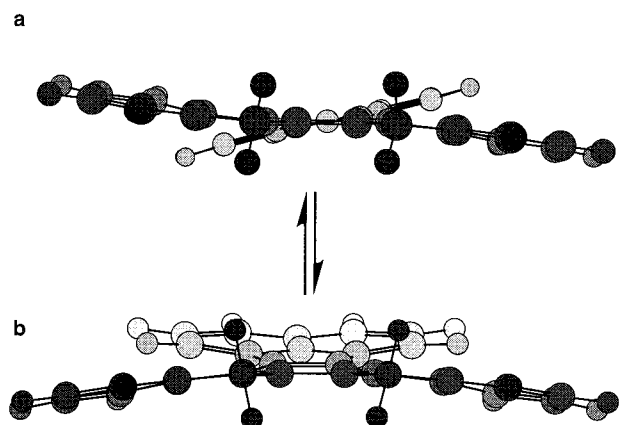
(24) Chipman, D. M. *Theor. Chim. Acta* **1992**, 82, 93–115.(25) Cramer, C. J. *J. Org. Chem.* **1991**, 56, 5229–5232.(26) Qin, Y.; Wheeler, R. A. *J. Phys. Chem.* **1996**, 100, 10554–10563.(27) (a) Niemz, A.; Rotello, V. M. *J. Am. Chem. Soc.* **1997**, 119, 6833–6836. (b) Bryce, M.; Moore, A.; Batsanov, A.; Howard, J.; Petty, M.; Goldenberg, L.; Williams, G.; Cuello, A.; Rotello, V. *J. Mater. Chem.* **1999**, 9, 2973–2978. (c) Rotello, V. *Heteroatom. Chem.* **1998**, 605–606.(28) Adamo, C.; Barone, V.; Fortunelli, A. *J. Chem. Phys.* **1995**, 102, 384–393.(29) Batra, R.; Giese, B.; Spichty, M.; Gescheidt, G.; Houk, K. N. *J. Phys. Chem.* **1996**, 47, 18371–18379.(30) Barone, V. *Theor. Chim. Acta* **1995**, 91, 113–128.

Table 2. Spin Delocalization in the Radical Anions **1**–**4**

PAH	total sd	core sd ^a	phenyl sd ^b	core sd / C $\times 10^2$ ^c	phenyl sd / C $\times 10^2$ ^c
1a	2.309	2.286	0.023	8.79	0.19
1b	2.278	2.256	0.022	8.68	0.18
2	2.393	2.393		9.20	
3	1.678	1.642	0.036	10.25	0.30
4	1.695	1.573	0.122	9.50	0.79

^a Total spin density resident in core. ^b Total spin resident on peripheral phenyls. ^c Total spin density/number of carbons. Spin density on protons and halogens <3%.

Scheme 1. Top View of the Tied Back Diphenyl Fluoranthene **4** Looking Down on the Methylene Protons along the Center Axis of the Molecule for the Twisted Conformer (a) in Thermal Equilibrium with Butterfly Conformer (b)



angles of $\sim 67^\circ$, considerably lower than those for the radical anions of **1a,b**. Even in this less conformationally restricted system, 98% of the spin density resides in the core fragment. Comparison of the spin density per carbon atom for the phenyl substituents indicates an approximately 50% increase for **3** compared to **1a,b**. This still amounts, however, to only 3% of the spin density per carbon seen for the core carbons.

The acenaphthofluoranthenes **1a,b** and **2** as well as fluoranthene **3** all represent symmetrical molecules of reasonably well-defined geometry. Computational hfc's derived from single-point calculations of the optimized geometries thus are found to be in overall good agreement with experimental results. No simple correlation, however, is possible between experimental and computational hfc's for the tied-back diphenylfluoranthene **4**. Geometry optimization of **4** resulted in two minimized conformations (Scheme 1), one with both phenyls up (butterfly), the other with one phenyl up, one down (twisted). Their comparable energy ($\Delta\Delta H = 0.614$ kcal/mol) allows for population of both conformers at room temperature, which is supported by molecular dynamics simulations showing interconversion between the two structures on the picosecond time scale.

Both conformers exhibit distinctly different spin density distributions, resulting in vibrational averaging of hfc's. In addition, the distortion lowers the symmetry of the molecule, further complicating correlation between computational and experimental hfc's. The agreement between experimental and computational hfc's for the core protons of **4**, however, justifies the use of computational results as approximation for the actual electronic structure. Single-point calculations for both conformers of **4** predict significant computational hfc's caused by the phenyl-protons, in agreement with experimental results. Analysis of the spin density distribution within the π -framework reveals that on average 7% of the total spin density resides in the phenyl

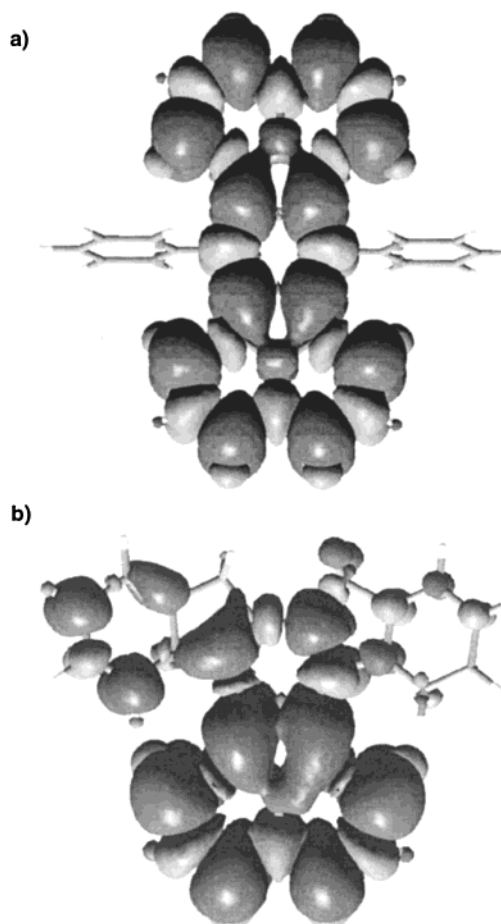


Figure 4. DFT-B3LYP 6-311G* spin density distribution for (a) the radical anion of **1a** and (b) the radical anion of **4** in the butterfly conformation.

substituents for the tied-back diphenyl fluoranthene **4**, compared to only 1% for the orthogonal diphenyl acenaphthofluoranthene **1a** and 2% for the less constrained diphenyl fluoranthene **3** (Figure 4).

Conclusions

The radical anions of the 7,14-diphenyl-substituted acenaphthofluoranthenes **1a,c** effectively confine the unpaired electron to the polycyclic core, due to a combination of the rigid orthogonal alignment of the σ -bonded π -systems and the low spin density at the sites of substitution. The confinement was found to be independent of further substitution on the phenyl rings. A gradual decrease in spin localization is observed as a function of decreasing dihedral angle in the radical anions of the 7,10-disubstituted fluoranthenes **3** and **4**.

7,14-Diphenyl-substituted acenaphthofluoranthenes are 2D-anisotropic systems with regards to their conductivity, capable of electron delocalization along the axis of the polycyclic core and electron confinement along the axis of the phenyl substituents. Extensive electron delocalization in the first dimension can be achieved through electropolymerization of these systems, which yields a ladder-type polymer due to carbon-carbon bond formation involving the naphthyl moieties.¹⁶ The bromo-system **1c** can be readily incorporated into phenylene-acetylene and other molecular wires, where it could act as a quantum well, in which an unpaired electron can be confined. 7,14-Diphenyl-substituted acenaphthofluoranthenes therefore provide intriguing prospects as building blocks in the context of molecular electronics.

Acknowledgment. This research was supported by the National Science Foundation (9905492) and the Petroleum Research Fund, administered by the American Chemical Society. V.R. acknowledges support from the Alfred P. Sloan Foundation, Research Corporation, and the Camille and Henry Dreyfus Foundation. We thank Prof. Paul Lahti for helpful discussions.

Supporting Information Available: Experimental and simulated SEEPR spectra of the radical anions of **1–4**, as well as simulation parameters and spin densities (PDF). This material is available free of charge via the Internet at <http://pubs.acs.org>.

JA9944148